

Selective Detection of Silver Ions by Self-assembled Monolayers of Electron-defect Bipyridine Derivatives

Zhen Zhang, Qi-Hua Jiang, Yi-Long Liu, Xiao-Qiang Sun, Yong Kong and Hai-Tao Xi*

Key Laboratory of Fine Petrochemical Engineering, Changzhou university, Changzhou, Jiangsu 213164, P.R. China

*E-mail: xihaitaocczu@gmail.com

Received: 21 January 2015 / Accepted: 12 February 2015 / Published: 24 February 2015

1,1''-(5-(3-(acetylthio)propoxy)-1,3-phenylene)bis(methylene))bis((4,4'-bipyridin)-1-ium) has been successfully synthesized by a straightforward reaction and its electrochemical properties of self-assembled monolayers (SAMs) on Au electrode are measured by cyclic voltammetry (CV) and electrochemical impedance spectroscopy (EIS). The barrier property of the SAMs-modified surface is evaluated by using potassium ferro/ferri cyanide. The results suggest that its SAMs can reduce the charge transfer resistance (R_{ct}) and accelerate the electron transfer rate. CV results showed that SAMs-modified Au electrode rapidly recognized Ag^+ and had excellent cycle stability. The structural and morphological information has also been obtained by field emission scanning electron microscope (FE-SEM), the Ag composition of SAMs was 15.53% which is much higher than other compounds we have ever got.

Keywords: SAMs, Cyclic voltammetry, Electrochemical impedance spectroscopy, Ion recognition

1. INTRODUCTION

The electroactive molecular self-assembled monolayers (SAMs) [1] modification of gold electrode has been applied to molecular recognition [2,3], ion recognition [4-6], sensors [7,8], biosensors [9], molecular motors [10], lithography [11,12], and anti-corrosion [13] technologies. Recently, SAMs of alkylthiols [14] on Au are extensively studied due to their dense structures with relatively high stability. They directly suppress electrochemical processes at the metal and solution interface with a minimal peak current and great impedance. These properties of alkylthiols SAMs make it a good candidate in anti-corrosion [13]. Electron-defect bipyridine derivatives have been used as electroactive molecular SAMs for electrode modification, which are different from the conventional inert SAMs of alkylthiols. With the positively charged monolayers of electron-defect bipyridine which

can not only accelerate the rate of electron transfer but also increase the active surface area of the electrode, the voltammetric detection of metallic cations can be accomplished easily.

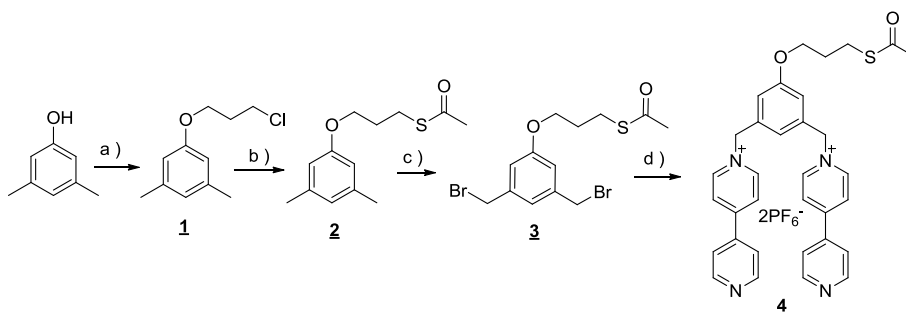
A variety of techniques, including X-ray photoelectron spectroscopy (XPS) [15], fourier transform infrared spectroscopy (FT-IR) [16,17], atomic force microscopy (AFM) [18], scanning tunneling microscopy (STM) [19,20], scanning electrochemical microscopy (SECM) [21], scanning electron microscopy (SEM) [22], Raman spectroscopy [23] and electrochemistry [5,24,25] are used to characterize the alkylthiol SAMs-modified electrodes. Electrochemical impedance spectroscopy (EIS) is an effective, nondestructive, informative and flexible technique to examine an electrochemical system, in which interfacial impedance of the electrode/solution is influenced by specific microscopic events of interest. An EIS sensor has been successfully applied in the detection of ascorbic acid in urine samples [26].

While more attention has been paid to aliphatic thiols and other electron-rich compounds, we attempt to investigate the unusual behaviors of organic electron-defect bipyridine derivatives SAMs. The bipyridine has a sulfide group rather than thiol or disulfide group which has usually employed in the SAMs preparation on gold surfaces. Though the sulfide group has lower bonding strength with gold, it's much stable than the thiol group in the presence of oxygen and will keep the bonding strength with gold. In this study, it is found that electron-defect bipyridine derivatives SAMs can accelerate the rate of electron transfer as well as increase the active surface area of the electrode. Moreover, it can be used to detect silver ions sensitively and selectively, which is proved by cyclic voltammetry (CV) and electrochemical impedance spectroscopy (EIS).

2. EXPERIMENTAL

2.1. Materials

We successfully synthesized 1,1''-((5-(3-(acetylthio)propoxy)-1,3-phenylene)bis(methylene))bis((4,4'-bipyridin)-1-ium)·2PF₆⁻ (**4**) (Scheme 1) for first time. All chemicals were analytical grade and used without further purification.



Scheme 1. Reagents and conditions: (a) 1-bromo-3-chloropropane, MeCN, reflux, 8 h, 98.5%; (b) potassium thioacetate, DMF, room temperature, 2 h, 95.5%; (c) NBS, AIBN, CCl₄, reflux, 3 h, 24%; (d) (i) 4,4'-bipyridine, MeCN, reflux, 18 h; (ii) NH₄PF₆, 50.5%.

The structure of key intermediates and target compound **4** were identified by melting point test,

^1H NMR and ^{13}C NMR [27].

2.2. Preparation of substrates

The gold disk electrode (CHI, 2mm in diameter) was pretreated using the following procedure prior to monolayer deposition. The electrode was cleaned in piranha solution, which is a mixture of 30% H_2O_2 and concentrated H_2SO_4 in 3:7 ratios. Then it was polished with alumina powder (diameter, 0.3 and 0.05 μm) followed by sonication in ethanol and deionized water. After copious rinsing with deionized water, the electrode was electrochemically cleaned by cycling the potential from -0.2 to +1.4 V at 50 mV/s in 0.5 M sulfuric acid until typical cyclic voltammogram of clean gold was obtained.^{21,22}

2.3. Preparation of SAMs and mixed SAMs

The pretreated gold electrode was immersed in 5 mmol/L **4** acetonitrile solution in darkness at 25°C for about 24 h. Then the modified electrode was removed from the solution and rinsed with deionized water and ethanol, and dried with high purity nitrogen. The SAMs-modified gold electrode was obtained and used for the electrochemical measurements immediately.

We had further tried to improve the blocking ability by forming a mixed SAMs with decanethiol. Immediately after the adsorption of corresponding compounds, the monolayer coated electrode was rinsed with deionized water and dipped in 10 mmol/L decanethiol-methanol solution for mixed SAMs formation. After 10 h at ambient temperature, the mixed SAMs modified electrode was rinsed with deionized water and dried with high purity nitrogen, and subsequently analyzed using electrochemical studies.

2.4. Electrochemical Measurements

Electrochemical measurements were conducted by a PC controlled CHI920C electrochemical workstation (CHI, Shanghai Chenhua Co). A conventional three-electrode electrochemical cell with a Pt wire as a counter electrode, a Ag/AgPF₆ (sat. KPF₆) electrode as a reference electrode and SAMs-modified gold electrode as working electrode was used for the electrochemical characterization of SAMs.

The structural and morphological information is obtained by field emission scanning electron microscope (FE-SEM, SUPRA55, Zeiss AG, Germany).

3. RESULTS AND DISCUSSION

3.1. Cyclic voltammetry

The electrochemical behavior of $[\text{Fe}(\text{CN})_6]^{3-/4-}$ at different modified electrodes can be revealed

by cyclic voltammetry (CV), which is an important electrochemical method used to assess SAMs (Figure 1). The redox peak current at **4**/Au is much larger than those at other modified electrodes (curve B), indicating that the electron transfer at **4**/Au is much easier. On the contrary, the morpholino-substituted thioacetate modified electrode has a lower redox peak current than the gold electrode [28] while compounds there are rich of electron. So, we can come to conclude that the larger redox peak current is mainly attributed to the electrostatic interaction between positively charged monolayer and negatively charged probe ($[\text{Fe}(\text{CN})_6]^{3-/4-}$). For the $\text{C}_{10}\text{SH}/\text{Au}$ electrode (curve D), no typical peak of the redox couple was observed. This might be ascribed to the

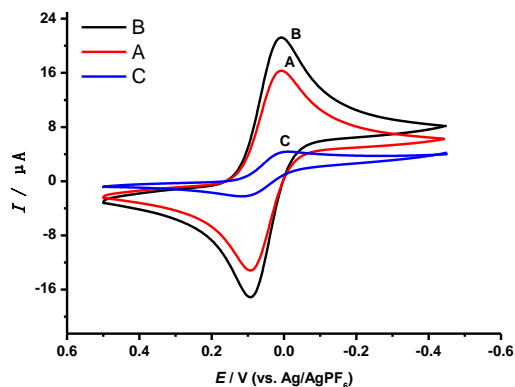


Figure 1. cyclic voltammograms of Au (A), **4**/Au (B), **4**/ $\text{C}_{10}\text{SH}/\text{Au}$ (C) in 5.0 mmol/L $\text{K}_3[\text{Fe}(\text{CN})_6]$ /0.1 mol/L KCl. Scan rate: 50 mV/s.

fact that C_{10}SH anchored on the surface of Au electrode assembled a highly ordered, compact monolayer which completely inhibited the redox reaction. However, it is interesting to find that there is still a pair of redox peaks observed when C_{10}SH is added to **4** SAMs (curve C). The differences between curve C and D indicate that the positively charged monolayer of electron-defect bipyridine derivatives can enhance the redox behavior of $[\text{Fe}(\text{CN})_6]^{3-/4-}$ probe, and SAMs of C_{10}SH can be a direct obstacle at the electrode-liquid interface.

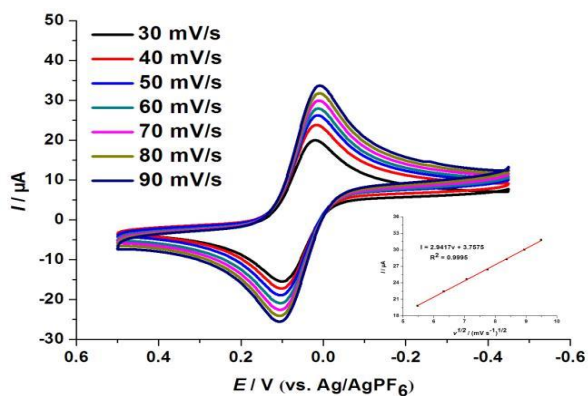


Figure 2. Cyclic voltammograms of **4**/Au in 5.0 mmol/L $\text{K}_3[\text{Fe}(\text{CN})_6]$ /0.1 mol/L KCl. Scan rate: 30, 40, 50, 60, 70, 80, 90 mVs^{-1} . Inset: $I_{\text{pc}}-v^{1/2}$.

Figure 2 showed the oxidation peak current is increased with increasing scan rate, meanwhile, the peak potential shifts positively. The corresponding inset of this figure showed that the anodic peak current (I_{pc}) had a direct linear relationship with the square root of scan rate. The linear regression equation were $I_{pc}=2.9417v^{1/2}+3.7575$ ($R^2=0.9996$), which demonstrating that the electron transfer process was essentially diffusion controlled.

According to the date obtained from the figure 2, we could calculate the electroactive surface area (A_a) and the absorption coverage (Γ) of the monolayer on the gold electrode using equations $I_{pa}=2.69 \times 10^5 n^{3/2} D^{1/2} A_a v^{1/2} c$ and $\Gamma=Q/nFA$ respectively (Table 1) [14]. (Where I_{pa} is anodic peak current, n is the number of electrons transferred ($n=1$), D is the diffusion coefficient ($D=7.6 \times 10^{-6} \text{cm}^2/\text{s}$) [29], A_a is the electroactive surface area, v is the san rate, c is the bulk concentration of an oxidant, Γ is the absorption coverage, Q is the estimated charge under the reduction or oxidation peak, F is the Faraday constant, and A is the geometric area of the gold electrode(0.0314cm^2)). From the calculated A_a and the surface coverage values, it was clear that the 4/Au had a lower blocking ability compared with the gold electrode.

Table 1. Some electrochemical values of Au and 4/Au in 5.0mmol/L $\text{K}_3[\text{Fe}(\text{CN})_6]$ /0.1 mol/L KCl. (A_a is the electroactive surface area, Γ is the absorption coverage, R_{ct} is the charge transfer resistance and θ is the surface coverage .)

Sample	$A_a(\text{cm}^2)$	$\Gamma/\text{mol} \cdot \text{cm}^{-2}(10^{-10})$	θ	R_{ct}/ohm
Bare Au	0.0181	2.398	-	188.1
4/Au	0.0203	2.701	0.13	160,4

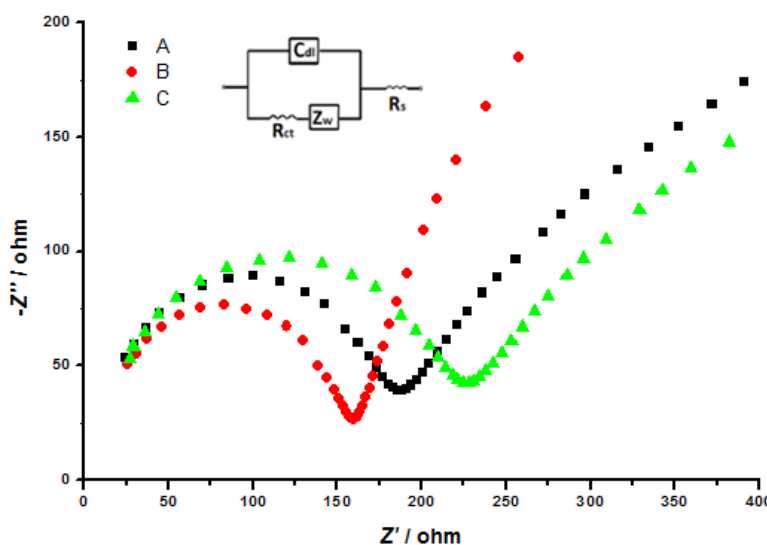


Figure 3. Impedance plots of Au(A), 4/Au(B), 4/C₁₀SH/Au (C), in 5.0mmol/L $\text{K}_3[\text{Fe}(\text{CN})_6]$ /0.1 mol/L KCl. Frequency range from 1 Hz to 1000 KHz at the open circuit potential of 0 V. Amplitude: 5 mV. Inset: the equivalent circuit used to model the experimental data.

3.2. Electrochemical Impedance Spectroscopy

EIS is a useful technique for analyzing the quality of SAMs on metal electrodes, as it provides quantitative information about the structural integrity of the monolayers and the influence of electrode/solution. Some parameters such as the charge transfer resistance of bare Au electrode (R_0) and the charge transfer resistance of the corresponding different SAMs-modified electrodes (R_{ct}) could be calculated from the figure 3. R_{ct} was a measure of blocking ability of the monolayer films towards the electron transfer reaction, higher the R_{ct} values better the blocking behavior of monolayers. For the **4**/Au, it could be seen the smaller semicircular diameter which indicated the faster electron transfer kinetics of $[\text{Fe}(\text{CN})_6]^{3-/4-}$ probe on modified electrode. The properties of gold electrode modified by decanethiol has been studied extensively [30]. It usually has a typical R_{ct} value up to several thousands Ohm [31], which indicated decanethiol has a good blocking ability for the redox reaction. It could also be noted from figure 3 that **4**/ C_{10}SH /Au showed a large impedance compared with the **4**/Au, but the impedance values were much lower than the electrode modified by decanethiol. We could know that the SAMs of compound **4** can accelerate the rate of electron transfer on the surface of the electrode, and the results were in conformity with our studies using cyclic voltammetry. Table 1 showed the R_{ct} values and the surface coverage (θ) of bare Au and **4**/Au obtained from the Nyquist plots.²⁶ Based on the equation: $\theta = 1 - (R_0/R_{ct})$, the surface coverage could be calculated by assuming that the current was attributed to the presence of pinholes within the monolayers. From the R_{ct} values and surface coverage (θ), there is no doubt that the **4** SAMs can reduce the charge transfer resistance (R_{ct}) and accelerate the electron transfer rate.

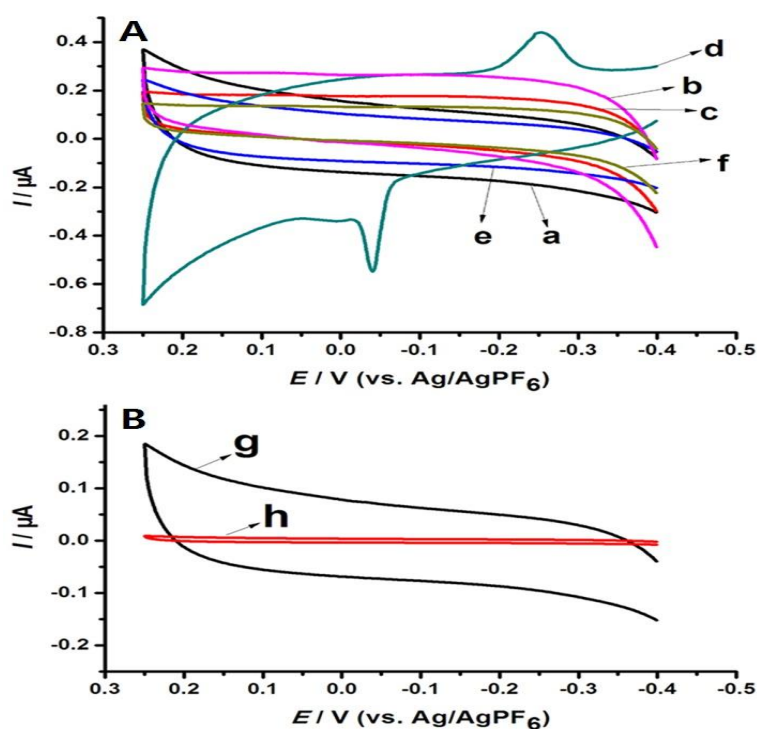


Figure 4. A: Co^{2+} (a), Mg^{2+} (b), Cu^{2+} (c), Ag^{2+} (d), Fe^{3+} (e), Pb^{2+} (f) at the SAMs of **4** on Au electrode in 0.1 mol/L KCl. B: the result of unmodified Au (g) and $\text{C}_{10}\text{SH}/\text{Au}$ (h) identified the ions. Scan rate: 50 mV/s.

3.3. Ion recognition

Unmodified Au, **4**/Au and C₁₀SH/Au were immersed in 1.0 mmol/L CoCl₂, MgCl₂, Cu(NO₃)₂, AgNO₃, FeCl₃ and Pb(NO₃)₂ solution respectively for 1 min followed by rinsing with deionized water. It could be seen from figure 4(B) that unmodified Au and C₁₀SH/Au could not identify those ions. In curve d of figure 4(A), **4**/Au enriched of Ag⁺ showed reversible redox peaks, indicating that Ag⁺ was adsorbed to the SAMs. In contrast, there were no obvious redox peaks of **4** SAMs enriched with Co²⁺, Mg²⁺, Cu²⁺, Ag²⁺, Fe³⁺ and Pb²⁺, so, they could not be absorbed to the SAMs. With 100-fold excess concentrations of Co²⁺, Mg²⁺, Cu²⁺, Fe³⁺, Pb²⁺, Zn²⁺, NH₄⁺ and NO₃⁻, the silver ion peak current only decreased by 5%, in a word, they could not interfere with the determination of 1.0 mmol/L silver ions and the presence of electrolyte (KCl) did not disturb the detection of silver ions[9], **4**/Au was found to be highly selective for sensing Ag⁺ over other metal ions. As for the mechanism of Ag⁺ was concentrated in electron-defect bipyridine derivatives, this might due to the lone electron pair of nitrogen and the π-π interactions of bipyridine (figure 5).

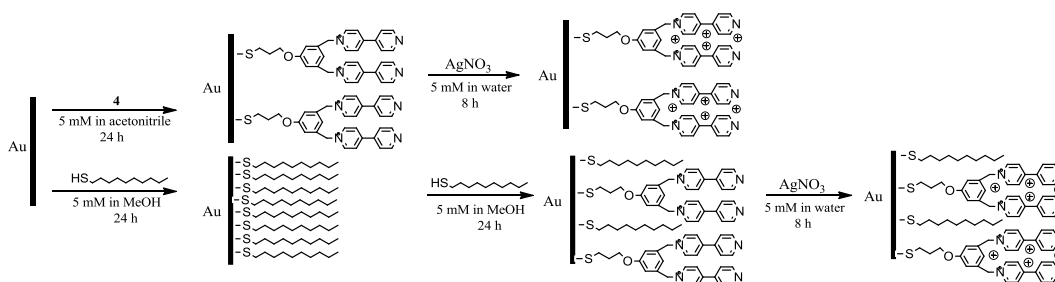


Figure 5. schematic representation of the proposed mechanism for the electron-defect bipyridine derivatives self-assembly process and the identification of silver ions.

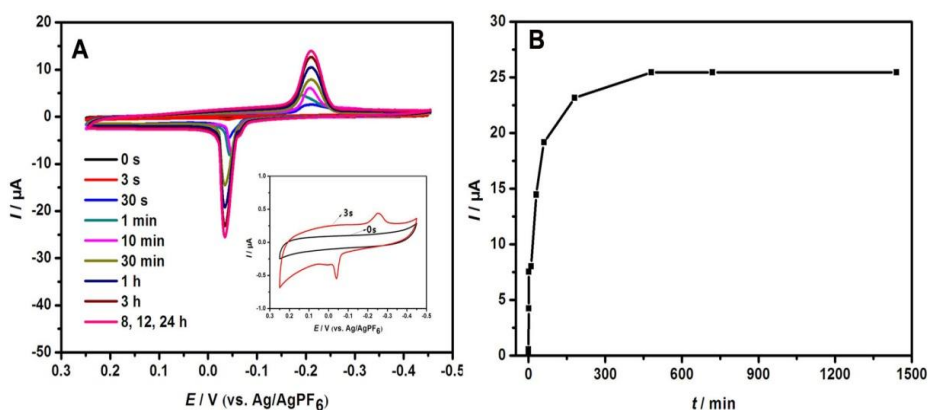


Figure 6. A: Cyclic voltammograms of **4**/Au electrode absorbed Ag⁺ in 0.1 mol/L KCl. Deposition time: 0 s, 3 s, 30 s, 1 min, 10 min, 30 min, 1 h, 3 h, 8 h, 12 h, 24 h. Inset: deposition time at 3 s. B: I_{pc}-t.

Cyclic voltammograms showed a reversible redox peak when the deposition time was 3 s (Figure 6A inset). The peak current enlarged as immersion time increasing, then, it plateaued after 8 h (Figure 6B). In our experiment, we found that the 1.0 μmol/L Ag⁺ needed 5 min for response and the

detection limit was 2.0 nmol/L (at least 3 h). The successful detection of Ag^+ in a short immersion time indicated that **4**/Au was highly sensitive in detecting Ag^+ . This developed electrochemical method enabled a very selective, fast, low cost detection of silver ions, with a higher sensitivity compared with that achieved by some biosensors [32] and potentialmetric sensors [33].

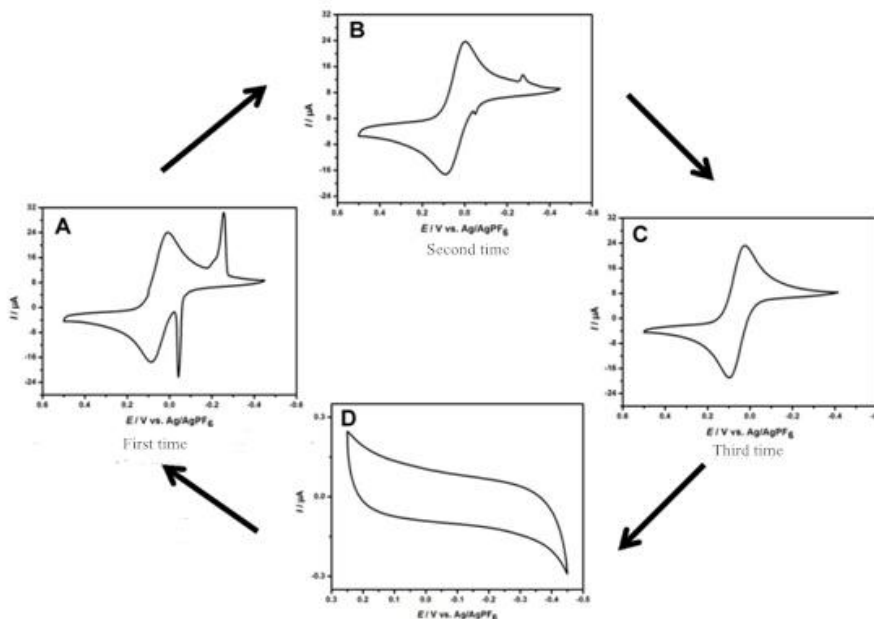


Figure 7. Cyclic voltammograms of **4**-Ag/Au in 5.0 mmol/L $\text{K}_3[\text{Fe}(\text{CN})_6]$ /0.1 mol/L KCl. The scanning cycles was three (A was the first time, B was the second time and C was the third). D: Cyclic voltammograms of **4**/Au in 0.1 mol/L KCl at the end of the experiment. Scan rate: 50 mV/s.

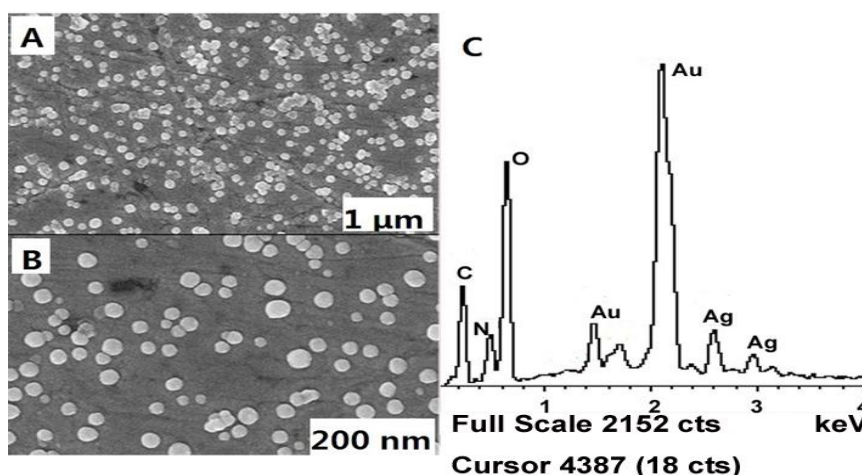


Figure 8. A and B: FE-SEM images of **4**-Ag/Au; C: EDS spectrum of **4**-Ag/Au.

4/Au was immersed in 1.0 mmol/L AgNO_3 for 5 min, then the electrode was removed from the solution and rinsed with deionized water. The cyclic voltammograms test was performed in 5.0

mmol/L $\text{K}_3[\text{Fe}(\text{CN})_6]$ /0.1 mol/L KCl and the scanning cycle was set at three. As could be seen from Figure 7A, there were two pair of redox peaks that appeared at **4**/Au. The oxidation peak was attributed to $[\text{Fe}(\text{CN})_6]^{3-/4-}$ at 84.2 mV and the redox peak due to Ag^+ was established at -0.05 and -0.3 V. Increasing the scanning cycle rapidly decreased the silver redox peak (Figure 7B). Furthermore, the silver redox peak eventually disappeared at the third time (Figure 7C). At the end of our experiment, we removed the electrode and rinsed it with distilled water, then we executed the cyclic voltammograms in 0.1 mol/L KCl. Unexpectedly, the silver redox peak remained non-existent (Figure 7D) and results showed that $[\text{Fe}(\text{CN})_6]^{3-/4-}$ made silver ions via stripping the molecular membrane. Furthermore, we saw that **4**/Au returned to its original state. Many tests found that the electrode could be recycled 8 to 10 times at room temperature which indicated that the **4**/Au electrode had excellent cycle stability.

In order to absorb the Ag^+ completely, **4**/Au was immersed in 1.0 mmol/L AgNO_3 for 8 h. Afterwards, a field emission scanning electron microscope (FE-SEM) was used to examine the general morphologies of **4**-Ag/Au. As could be seen from Figure 8A, there are many nanoparticles distributed on the surface of Au electrode uniformly. Then we magnified the image in 200 nm (Figure 8B), it is clearly to see the morphology of the nanoparticle like a irregular dot and the surface coverage of Au electrode was in a low degree. Figure 8C showed the EDS spectrum of SAMs of **4**-Ag, the Ag composition of it was 15.53%, which is much higher than that of the electron-rich compounds [28]. It indicated that the electron-defect bipyridine derivatives showed a high performance in recognition for silver ions.

4. CONCLUSION

In this study, this electron-defect bipyridine derivative is reported for the first time as a probe for silver ion sensing, the electrochemical experiments showed the great selectivity and high sensitivity in recognition for Ag^+ . Due to electrostatic interaction between positively charged monolayer and negatively charged probe, the **4** SAMs modified electrodes increased the electroactive surface area and accelerated the electron transfer. From the cyclic voltammograms of **4**/Au, it has an apparent and fast capacity in recognition for Ag^+ and the electrode could also be used repeatedly upwards of 8 to 10 times. Under the optimum conditions, the sensor showed a low detection limit of 2.0 nmol/L, This sensitive detection of Ag^+ was attributed to the π - π interactions of bipyridine and the lone electron pair of nitrogen atom. In a word, the electron-defect bipyridine derivatives showed a lot of advantages over the electron-rich compounds in many aspects. Electron-defect bipyridine derivatives modified Au electrode presented tremendous potential for detecting silver ions in polluted water, and it might be a suitable sensor for the detection of silver ions in serum protein.

ACKNOWLEDGEMENTS

The authors are grateful for the financial support from the National Natural Science Foundation of China (No. 20872051).

References

1. S. H. Gyepi-Garbrah and R. Šilerová, *Phys. Chem. Chem. Phys.*, 4 (2002) 3436-3442.
2. X. P. He, X. W. Wang, X. P. Jin, H. Zhou, X. X. Shi, G. R. Chen and Y. T. Long, *J. Am. Chem. Soc.*, 133 (2011) 3649-3657.
3. W. Su, M. Cho, J.-D. Nam, W.-S. Choe and Y. Lee, *Electroanalysis*, 25 (2013) 380-386.
4. R. K. Shervedani and S. Pourbeyram, *Biosens. Bioelectron.*, 24 (2009) 2199-2204.
5. G. Trippe', M. Ocafrain, M. Besbes, V. Monroche, J. Lyskawa, F. L. Derf and M. Salle', *New J. Chem.*, 26 (2002) 1320-1323.
6. R. Rawal, S. Chawla, P. Malik and C. S. Pundir, *Int. J. Biol. Macromol.*, 51 (2012) 175-181.
7. R. K. Shervedani, A. Farahbakhsh and M. Bagherzadeh, *Anal. Chim. Acta*, 587 (2007) 254-262.
8. R. Shervedani and S. Pourbeyram, *Sens. Actuators, B*, 160 (2011) 145-153.
9. C. Hu, D.-P. Yang, Z. Wang, P. Huang, X. Wang, D. Chen, D. Cui, M. Yang and N. Jia, *Biosens. Bioelectron.*, 41 (2013) 656-662.
10. H.-R. Tseng, D. Wu, N. X. Fang, X. Zhang and J. F. Stoddart, *Chem. Phys. Chem.*, 5 (2004) 111-116.
11. M. E. Anderson, C. Srinivasan, J. N. Hohman, E. M. Carter, M. W. Horn and P. S. Weiss, *Adv. Mater.*, 18 (2006) 3258-3260.
12. J. L. Tan, J. Tien and C. S. Chen, *Langmuir*, 18 (2002) 519-523.
13. C.-T. Wang, S. Chen, H. Ma, L. Hua and N.-X. Wang, *J. Serb. Chem. Soc.*, 67 (2002) 685-696.
14. S.-J. Ding, B.-W. Chang, C.-C. Wu, M.-F. Lai and H.-C. Chang, *Anal. Chim. Acta*, 554 (2005) 43-51.
15. K. S. Lokesh, K. D. Wael and A. Adriaens, *Langmuir*, 26 (2010) 17665-17673.
16. C. M. Pandey, G. Sumana, K. N. Sood and B. D. Malhotra, *Thin Solid Films*, 519 (2010) 1178-1183.
17. A. Hamzehloei, M. F. Mousavi and S. Z. Bathaie, *Electroanalysis*, 24 (2012) 1362-1373.
18. I. Kaur, X. Zhao, M. R. Bryce, P. A. Schauer, P. J. Low and R. Katakay, *Chem. Phys. Chem.*, 14 (2013) 431-440.
19. S. Y. Lee, Y. Choi, E. Ito, M. Hara, H. Lee and J. Noh, *Phys. Chem. Chem. Phys.*, 15 (2013) 3609-3617.
20. W. Zhou, T. Baunach, V. Ivanova and D. M. Kolb, *Langmuir*, 20 (2004) 4590-4595.
21. W. Sanders and R. Vargas, *Langmuir*, 24 (2008) 6133-6139.
22. R. Rawal, S. Chawla, P. Malik and C.S. Pundir, *Int. J. Biol. Macromol.*, 51 (2012) 175-181.
23. K. Nishiyama, A. Kubo, A. Ueda and I. Taniguchi, *Chem. Lett.*, 31 (2002) 80-81.
24. Y. Q. Zhao, H. Q. Luo and N. B. Li, *Sensors and Actuators B*, 137 (2009) 722-726.
25. Y. D. Wang, Y. Bai, M. S. Liang and W. J. Zheng, *Electroanalysis*, 21 (2009) 2145-2152.
26. S. Qiu, S. Gao, Q. Liu, Z. Lin, B. Qiu and G. Chen, *Biosens. Bioelectron.*, 26 (2011) 4326-4330.
27. Spectra of four compounds are summarized as follows: Compound 1: ^1H NMR (300 MHz, CDCl_3) δ : 2.17-2.25 (m, $J = 6.0$ Hz, 2H), 2.28 (s, 6H), 3.71-3.75 (t, $J = 6.0$ Hz, 2H), 4.05-4.09 (t, $J = 6.0$ Hz, 2H), 6.54 (s, 2H) 6.60 (s, 1H); compound 2: ^1H NMR (300 MHz, CDCl_3) δ : 1.99-2.07 (m, $J = 6.0$ Hz, 2H), 2.28 (s, 6H), 2.33 (s, 3H), 3.02-3.07 (t, $J = 6.0$ Hz, 2H), 3.94-3.98 (t, $J = 6.0$ Hz, 2H), 6.52 (s, 2H), 6.59 (s, 1H); compound 3: ^1H NMR (300 MHz, CDCl_3) δ : 2.03-2.11 (m, $J = 6.0$ Hz, 2H), 2.35 (s, 3H), 3.03-3.07 (t, $J = 6.0$ Hz, 2H), 4.00-4.04 (t, $J = 6.0$ Hz, 2H), 4.43 (s, 4H) 6.85 (s, 2H), 7.00 (s, 1H); compound 4: mp: 188.9-190.4°C. ^1H NMR (300 MHz, DMSO-d_6) δ : 1.92-2.01 (m, $J = 6.0$ Hz, 2H), 2.31 (s, 3H), 2.94-2.99 (t, $J = 6.0$ Hz, 2H), 4.02-4.06 (t, $J = 6.0$ Hz, 2H), 5.82 (s, 4H), 7.26 (s, 3H), 8.02-8.04 (d, $J = 6.0$ Hz, 4H), 8.64-8.66 (d, $J = 6.0$ Hz, 4H), 8.88-8.90 (d, $J = 6.0$ Hz, 4H), 9.28-9.30 (d, $J = 6.0$ Hz, 4H). ^{13}C NMR (75 MHz, DMSO-d_6) δ : 25.64, 29.11, 31.04, 63.02, 67.01, 116.36, 121.67, 122.40, 126.21, 136.93, 141.18, 145.91, 151.50, 153.37, 159.78, 195.66.
28. Jian .Jin, Ying. Chen and Yi-L. Liu, *Bull. Korean Chem. Soc.*, 35 (2014) 601-604.

29. B. Roffel and J. J. v. d. Graaf, *Journal of Chemical and Engineering Data*, 22(1977) 300-302.
30. Finklea, H. O.; Snider, D. A.; Fedyk, J. *Langmuir*, 9 (1993) 3660-3667.
31. Richard. P. Janek and W. Ronald. Fawcett, *Langmuir*, 14 (1998) 3011-3018.
32. Abdullah. Affrose and Kasi. Pitchumani etc, *Sensors and Actuators B*, 206 (2015) 170-175.
33. Z. X. Wang and S. N. Ding, *Anal. Chem*, 86 (2014) 7436-7455.

© 2015 The Authors. Published by ESG (www.electrochemsci.org). This article is an open access article distributed under the terms and conditions of the Creative Commons Attribution license (<http://creativecommons.org/licenses/by/4.0/>).